2400 *Macromolecules* **1997,** *30,* 2400−2407

Raman Vibrational Studies of Syndiotactic Polystyrene. 2. Use of the Fundamental ν_1 Vibrational Mode as a Quantitative Measure of Crystallinity within Isotropic Material

Ewen J. C. Kellar,[†] Angus M. Evans, Johnathan Knowles,[‡] Costas Galiotis,* and Edgar H. Andrews

Department of Materials, Queen Mary and Westfield College, University of London, Mile End Road, London E1 4NS, U.K.

Received July 30, 1996; Revised Manuscript Received November 18, 1996[⊗]

ABSTRACT: Syndiotactic polystyrene (sPS) has been found to exhibit two distinct vibrational peaks in the Raman spectrum corresponding to the ν_1 vibrational mode. These features have been assigned to the symmetric phenyl ring breathing mode coupled to the polymer backbone. It has been shown that the presence of long all-*trans* sequences gives rise to a peak at ~773 cm^{-1}, whereas less well-defined *trans*/*gauche* conformations result in a separate peak at ~798 cm^{-1}. With increasing levels of crystallinity, the integrated intensity of the former feature grows at the expense of the high-frequency feature. The use of a series of annealed isotropic films of glassy sPS of increasing crystallinity and molten sPS has made it possible to examine the precise relationship between these two features and other neighboring vibrational peaks. The level of crystallinity within each sample has been determined independently using wide-angle X-ray scattering, differential scanning calorimetry, and infrared spectroscopic measurements. It has been found that the relative area under the all-*trans* ν_1 band can be directly related to the crystalline volume fraction within each sample. It is proposed that this Raman vibrational feature centered around 773 cm^{-1} can be used as a quantitative measure of crystallinity for sPS once the contribution from the all-*trans* sequences in the melt is subtracted from the spectrum.

Introduction

Polymers which exhibit the ability to crystallize have been the subject of much scrutiny for many years. The crystalline structure is morphologically and mechanically very different from that of amorphous material and can offer advantages in terms of solvent resistance, melting temperature, structural integrity, and mechanical performance.[1] Except in very carefully controlled conditions, polymers which crystallize only do so to a limited extent, resulting in a mixture of crystalline and amorphous domains, which can be regarded to some degree as a two-phase system. The relative proportion of these phases is therefore an important parameter to establish.

It is common knowledge that the "degree of crystallinity" of a semicrystalline polymer can be affected by the experimental technique employed for measurements. Two of the most widely used quantitative methods for assessing crystallinity are wide-angle X-ray diffraction scattering (WAXS) and differential scanning calorimetry (DSC). The former has the advantage of being nondestructive and highly effective for samples of high to intermediate crystallinity. However, the accuracy of the method is considerably diminished for samples of low crystallinity or of poor long-range order (poorly formed and/or very small crystallites).[2,3] In order to determine a value for the crystalline fraction, the assumption is made that the WAXS spectrum is composed of two superimposed spectra arising from the amorphous phase and crystalline phase, respectively.[2,3] For highly crystalline materials, this assumption largely holds true, and an amorphous background can be estimated and subtracted from the spectrum to give the crystalline contribution. However, polymers of intermediate crystallinity as described above give rise to poorly defined spectra with weak broad features from which the contribution of the amorphous phase is difficult to estimate. Other potential complications of WAXS arise from its relative large sampling depth (~300 μm) and its sensitivity to material anisotropy.[2,3]

DSC measures the heat of fusion of the sample and therefore can be termed as destructive. Its main advantages are the extremely small volumes of material required, the speed at which the experiment can be carried out, and its sensitivity to any level of long-range order. Unlike WAXS, DSC is insensitive to material orientation and requires a sample of almost negligible thickness. However, as is well known, the rate at which the sample is heated up or cooled down can give rise to errors in the measured crystalline volume fraction; e.g., a slow heating rate can result in subsequent recrystallization of the polymer during the scan, which results in an overestimate of crystallinity.[4,5] This phenomenon can be further complicated if the polymer under scrutiny is polymorphic, which may result in further multiple peaks which can be difficult to assign.[6−8]

Two further methods for qualitative crystallinity determination are density measurements and solvent uptake. Density measurements are nondestructive, orientation insensitive, and not limited by crystallite size but they do require a fairly large sample for an accurate value to be obtained. It is also necessary to know the reference density of the pure amorphous and the fully crystalline material.[9] Solvent uptake, on the other hand, is destructive and the assumption is made that the crystalline domains are unaffected by the solvent, whereas the amorphous region can be easily penetrated. The sample under study must be relatively large and have a high surface area to volume ratio to ensure complete solvent penetration. The accuracy of this technique suffers from the potential exclusion of the ordered (but not crystalline) interface region around each crystallite, as it may be susceptible to solvent attack.[10]

[†] Present address: TWI, Abington Hall, Abington, Cambridge CB1 6AL, U.K.

* Author to whom correspondence should be addressed (e-mail c.galiotis@qmw.ac.uk).

[‡] IRC in Biomedical Materials, QMW.

[⊗] Abstract published in *Advance ACS Abstracts,* March 15, 1997.

S0024-9297(96)01136-9 CCC: $14.00

The application of vibrational spectroscopic techniques to assess polymer crystallinity has been in existence for many years.[11,12] In principle, infrared and Raman spectroscopy should be able to provide useful data for polymer samples over the whole range of crystallinity. The experiments are fast and nondestructive. The primary aspect behind these methods is identification of spectral features which change in intensity, bandwidth, and/or position with crystallinity.[12,13] Most often these observations arise from conformational changes within the polymer backbone involving *trans* and/or *gauche* states. Polymers containing methylene sequences, for example, often crystallize in the fully extended *trans* conformation but care must be taken not to overlook any *trans* contribution found in the amorphous phase.[14]

As is well known, vibrational spectroscopy per se can only provide information for one-dimensionally-ordered chains. Hence, the appearance with molecular order of a band in the IR and/or Raman spectrum of a polymer can only be quantified by using some internal reference. To date, most work has been carried out using infrared spectroscopy on semicrystalline polymers, such as polyethylene (PE),[11] poly(ethylene terephthalate) (PET),[14] polypropylene (PP),[15] and nylon 6,6.[16] Most recently, developments in laser Raman instrumentation have enabled Raman spectroscopy to be used alongside infrared as a routine and complementary technique. Furthermore, Raman spectroscopy has the added advantage of using visible light, which can be focused to a spot size of ~1 μm, a distinct advantage over infrared spectroscopy, where the spot size is limited to 10–15 μm.

The vast bulk of crystallinity determination using Raman spectroscopy has been centered around PE.[11,17,18] The first truly quantitative study was published by Strobl and Hagedorn in 1978.[11] By examining spectra of molten, extended chain and semicrystalline, branched PE, they identified key spectral areas, which could be used to estimate quantitatively the proportion of extended all-*trans* chain material present within a semicrystalline sample. Furthermore, it was found that the spectral region corresponding to the methylene bending vibration (1510–1390 cm^{-1}) indicated that a third phase was present, which could be attributed to the interfacial region between crystalline and amorphous phases. Use of an internal standard peak enabled this region to provide the relative proportions for all three phases. This was corroborated through the use of wide-angle and small-angle X-ray scattering analysis and density studies over a range of temperatures. Naylor et al.[17] verified the notion of a two-phase model in PE by carrying out studies on a number of samples by means of FT-Raman and “dispersive” Raman spectroscopies. They concluded, however, that quantification of a third, intermediate phase is not possible when based on “dispersive” Raman spectra, due to the difficulty in fitting the complicated overlapping spectral features in the relevant spectral ranges.

PET has recently been under scrutiny by Rodriguez-Cabello et al.,[14] who have successfully demonstrated that Raman spectroscopy can be used in a quantitative fashion when measuring crystallinity. Spectral features were identified as being unique to the *trans* and *gauche* conformations within the ethylene glycol fragment. X-ray studies have shown that such a conformation is present within the crystalline state, whereas in the amorphous state the fragment has a more complicated conformational composition where both *trans* and *gauche* conformations can be present. By annealing the sample over a range of temperatures, a relationship was established between the features corresponding to the *trans* and *gauche* conformations. Analogous studies carried out using DSC enabled the proportion of *trans* conformations present in the amorphous phase to be ascertained (15%) and the true proportion of crystalline *trans* conformations to be determined. Comparison of the percent *trans* value with the percent crystallinity as determined from DSC showed an almost complete correlation. Further observations regarding the two-stage crystallization process during annealing of PET were also made by means of laser Raman spectroscopy.

Syndiotactic Polystyrene: Background

Since the announcement of the synthesis of syndiotactic polystyrene (sPS) in 1986,[20] considerable interest has been given to this material mainly because of its propensity to crystallize.[1,20–32] At least four distinct polymorphs (α, β, γ, and δ) have been identified, which can be grouped into two pairs according to the backbone conformation.[21,22] One pair (α, β) have a planar all-*trans* “zigzag” conformation whereas the other pair (γ, δ) have a helical *trans*–*trans*, *gauche*–*gauche* conformation.[23] Such variation in crystalline structure has prompted a number of vibrational spectroscopic studies on sPS.[24–32] The first observation to be made was of the presence of a peak at 1222 cm^{-1} in the infrared spectrum which was assigned to the presence of the planar conformation.[20]

Raman studies reported previously in the first part of this series[32] have identified the potential usefulness of the ν_1 vibration in backbone conformation analysis and in crystallinity determination. We have confirmed the observation made by Kobayashi et al.[31] that the ν_1 vibration is very sensitive to the local backbone conformation resulting in the presence of two distinct peaks at 770–773 and 796–802 cm^{-1} corresponding to all-*trans* conformations and mixed *trans*/*gauche* conformations, respectively. This assignment is further corroborated by work done by Jasse et al.,[33] where infrared and Raman studies were carried out on two model polystyrene compounds, 2,4-diphenylpentane and 2,4,6-triphenylheptane.

In the second part of this series on the use of Raman spectroscopy to study sPS, we have produced a range of samples of increasing crystallinity in order to establish a clear relationship between the two ν_1 vibrational peaks in terms of the ratio of the areas underneath each fitted curve, $R(A)$. This relationship is in turn used to show that the relative area occupied by the 773 cm^{-1} band vis-à-vis the combined area for the two ν_1 features can be used as a quantitative measure of crystallinity provided that the contribution from the melt is taken into account. This relationship is further borne out through comparison with data derived from DSC, WAXS, and infrared studies carried out on the same samples.

The samples were created by annealing films of glassy sPS above T_g for varying lengths of time so that each sample gave a different $R(A)$ value ranging from 0.29 (glass) to 1.9 (crystalline). Crystallinity was then derived for each sample using DSC (two scan rates) and WAXS techniques, thus enabling a direct comparison between the Raman vibrational data and the two analytical methods.

Infrared spectroscopy was also employed in this work, with crystallinity being calculated by means of relation-

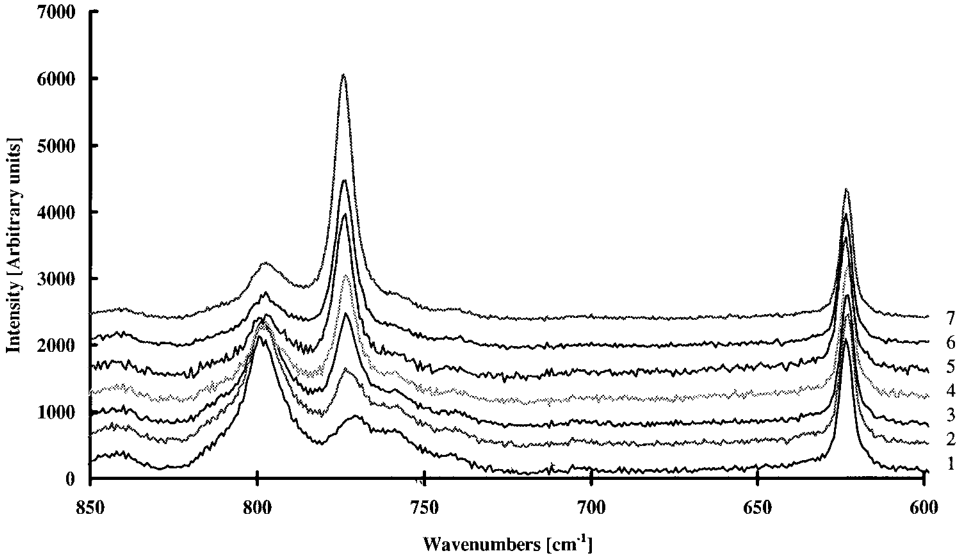

Figure 1. Raman spectra of progressively more crystalline (1−7) annealed sPS films.

ships cited by other groups. Vittoria et al.[10] have carried out extensive analysis of the intensity of the 1183 and 1222 cm^{-1} peaks and found a linear relationship between the ratio of peaks at 1222 and 1183 cm^{-1} ($I_{1222\ cm^{-1}}/I_{1189\ cm^{-1}}$) and the degree of crystallinity, as derived from chloroform absorption experiments. The peak at 1183 cm^{-1} in this case is used as a reference feature, since its intensity has been shown to be constant. Recently, Lopez et al.[34] have reported a similar relationship between bands at 1333 and 1377 cm^{-1}, with the latter feature being used as a reference. Both methods have been used to derive crystallinity values for the samples, enabling a useful comparison to be made.

The data from all four techniques have been analyzed and compared, enabling the effectiveness of each technique for samples of differing levels of crystallinity to be assessed. It has been found that values derived for low and intermediate crystallinities vary considerably between techniques and that use of a crystallinity index derived by Raman spectroscopic studies would appear to be the most consistent direct method for determining crystallinity for sPS. Hence, it is proposed to use Raman spectroscopy as a *quantitative* measure of crystallinity for sPS without necessarily resorting to other techniques.

Experimental Methods

Sample Preparation. Syndiotactic polystyrene with a weight-average molecular weight of 200 000 g mol^{-1} was used. The material was supplied in the form of quenched extruded sheets (thickness ~ 250 μm) which were optically transparent, isotropic (from Raman spectroscopic measurements and polarized optical microscopy) and was estimated to have a crystallinity of ~15−18% as derived by DSC. Such crystallinity levels are quite normal for "glassy" sPS as it has been virtually impossible to create zero-crystallinity material due to the high rate of crystallization of sPS. Seven samples were used in total and all the samples with the exception of the first (no. 1, control) and the last (no. 7, annealed at 160 °C for 90 min) were annealed for increasing lengths of time at 125 °C. Samples 2−6 exhibited decreasing levels of transparency whereas sample 7 had scattering characteristics intermediate to those of samples 5 and 6. Spectra were also taken of molten sPS in order to ascertain the relative intensities of the peaks of interest for a completely amorphous system.

Laser Raman Spectroscopy. Raman spectra were taken with the 514.5 nm line of an argon ion laser. A modified Nikon microscope was used to focus the incident laser beam onto the specimens. A 50× microscope objective of numerical aperture of 0.55 was employed. The laser spot was defocused into the sample to produce a sampling "cone" of diameter ~10 μm at the surface and ~2 μm within the sample. Sampling such a volume enables a more average spectrum to be collected. Eight spectra were collected for each sample on a random basis around the sample surface, and further "core" spectra were collected from a polished section in order to check for possible surface effects. The 180° backscattered light was collected by the microscope objective and focused on the entrance slit of a SPEX 1877 triple monochromator. A Wright Instruments MPP Peltier-cooled charge-coupled device (CCD) was employed for recording the Raman spectra. In order to achieve an improved signal to noise ratio, 12 spectra were collected from each sample and co-added together. The raw data were positionally calibrated with the use of the 622 cm^{-1} peak, and spectral analysis was carried out by fitting Lorentzian curves to the rest of the spectrum.

Fourier Transform Infrared (FTIR) Studies. Infrared studies were carried out with a Nicolet 730 FTIR spectrometer. The resolution was 2 cm^{-1}, and 50 scans were co-added to obtain a spectrum for each sample. Transmission spectra were obtained from the samples which had been ground and polished to a section of thickness of ~60 μm and area ~14 mm^2. The spectral window of interest (1000−1400 cm^{-1}) was plotted and a baseline drawn by visual inspection. The intensities of peaks at positions 1183, 1222, 1333, and 1377 cm^{-1} were measured and analyzed appropriately.

Differential Scanning Calorimetry (DSC). DSC studies were carried out with a Perkin-Elmer DSC-2C2, purged with nitrogen, with data reduction being performed by Perkin-Elmer software on a 3600 data station. The sample size was approximately 10 mg. Two scan rates were selected, 20 and 80 °C/min, to assess the effect of recrystallization within the material during the scan (50−300 °C). For crystallinity measurements, a heat of fusion of 53.2 J/g was assumed for 100% crystalline sPS.[36]

Wide Angle X-ray Scattering (WAXS). X-ray diffraction patterns were obtained from the center surface area of samples by means of a Siemens D5000 diffractometer. The samples were analyzed in flat-plate geometry with Cu Kα radiation and a graphite diffracted beam monochromator. A 2θ step of size 0.02° at every 12 s was used from 5 to 110°.

Results and Discussion

Laser Raman Spectroscopy (LRS). The Raman spectra of the seven annealed samples studied are presented in Figure 1. For clarity, the background has been subtracted and the spectral baselines are offset in

Table 1. Vibrational Assignments for Syndiotactic Polystyrene within the 600−800 cm^{-1} Region of the Raman Spectrum

Herzberg	ν_{18}	?	ν_8		ν_4	ν_2	ν_2		ν_{11a}
Wilson	ν_{6b}	?	ν_4	$\nu_{10b} + \nu_{16b}$	ν_{11}	ν_1 (tt...)	ν_1 (t/g...)	$\beta_{as}CH_2$	ν_{10a}
sPS-*trans* (crystal)	622		703	740	756	773	796	811	841
sPS (glass)	622	636	699	741	757	770	798	811	841

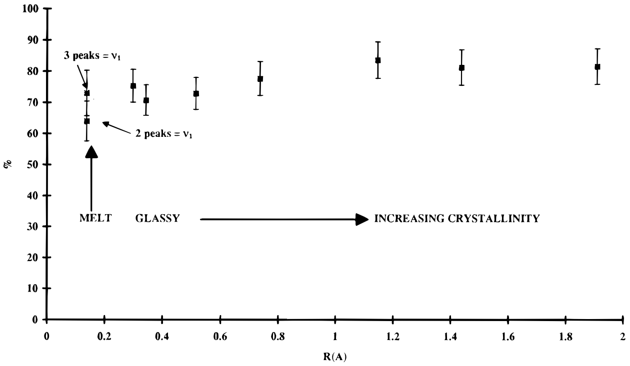

Figure 2. Variation of total area for the ν_1 vibration within the spectral envelope (700−800 cm^{-1})

order to produce a clear indication of the changes caused by the annealing process. Due to the changing scattering nature of the material upon annealing, the absolute intensities of the data were found to vary. A scaling factor was therefore applied to each spectrum derived from the integrated intensity of the 622 cm^{-1} feature. This peak (the ν_{6b} vibrational mode) was found to be unaffected in terms of its position and intensity by the morphology or degree of crystallinity within sPS, thus making it an ideal reference spectral feature for this material.

Previous work[32] has shown that the spectral area between 600 and 850 cm^{-1} consists of seven primary features, six of which are fundamental vibrational modes and 3−4 minor features. The appropriate assignments are given in Table 1. The primary peaks of interest, derived from the ν_1 mode, are the main features in an envelope from 720 to 820 cm^{-1}. In order to ascertain the relationship between these two peaks and the degree of crystallinity, the envelope was carefully analyzed by employing various curve-fitting routines. It has been demonstrated in the first paper of this series[32] that the ratio of the areas (R(A)) under the two ν_1 features changes from ∼0.29 to ∼1.9 as one moves from a glassy material to a crystalline one. As shown in Figure 2, the summed area relative to the total area under the 710−820 cm^{-1} envelope is shown to remain almost constant (77 ± 7%). A slight decrease is observed at lower levels of crystallinity but this effect can be attributed to fitting errors due to the weakness of the all-*trans* feature and associated poor signal to noise ratio. These results strongly suggest that the relative proportion of the intensities of these peaks is related directly to conformational transitions between an all-*trans* to *trans*/*gauche* backbone within the material.

The spectrum of molten sPS also shows a similar profile (Figure 3); however, it differs from the other spectra in that an extra band must be fitted at 768 cm^{-1}. Raman studies of sPS during melting and annealing confirm the presence of a third feature within the ν_1 envelope only in the molten state. This feature appears initially as a shoulder of the all-*trans* ν_1 peak and disappears rapidly as the material starts to crystallize.[36] It has not been possible to fit this extra feature to the spectra of solid sPS irrespective of form and, thus, it currently remains unassigned. However, when the total ν_1 area is compared to the area under the complete envelope (710−820 cm^{-1}) for all the samples (Figure 2), there is a strong indication that it can be assigned as a component of the ν_1 vibrational mode. If the band is excluded from this assignment, the total ν_1 contribution relative to the intensity of the whole envelope appears to be rather low.

The present work involved the annealing of amorphous, unoriented, stress-free films. The ν_1 vibrational mode is basically a phenyl ring breathing mode coupled to the polymer backbone.[32] Molecular modeling work performed on sPS[35] has shown that it is virtually impossible—due to steric hindrance—to form isolated *trans* segments. Such segments can only be formed by the mutual cooperation of adjacent chains in a three-dimensional space. Indeed, optical microscopy and the considerable narrowing of the 773 cm^{-1} bandwidth with isothermal annealing (Figure 1) provide further evidence for the development of crystallization in these unoriented films. Finally, as has been shown earlier, the development of 3D crystalline order in sPS is favored both thermodynamically and—in certain cases—by the kinetics of the crystallization process.[21−23]

It is concluded, therefore, that the relative integrated area of the all-*trans* feature at ∼773 cm^{-1} can be related quantitatively to the proportion of an all-*trans* phase within sPS and, hence, to crystalline volume fraction. However, the spectrum from molten sPS suggests that there is a residual component of all-*trans* conformations (∼12%) within the amorphous material, as would be expected statistically. This broad feature is clearly evident (Figure 3) and is centered around 777 cm^{-1}. It is therefore important to subtract the intensity of the 777 cm^{-1} band, I_{777}^{melt}, from the intensity of the 773 cm^{-1} band, I_{773}, which encompasses all trans−trans sequences. Thus, the amount of crystallinity, x_c, can be calculated from the formula

$$x_c = \frac{I_{773} - I^{\text{melt}}{}_{777}}{I_{773} + I_{796}} \tag{1}$$

where I_{796} is the total integrated intensity of amorphous non-*trans* sequences. The percentage of crystallinity calculated by Raman spectroscopy, $\%_{773}$, is thus given by

$$\%_{773} = 100x_c \tag{2}$$

The values of crystallinity of annealed films derived by means of Raman spectroscopy ($\%_{773}$) are now compared with those derived by WAXS, DSC, and infrared spectroscopy (Table 2) to critically assess the various methods employed for crystallinity measurements.

Wide-Angle X-ray Diffraction (WAXS). The WAXS traces for samples 1−7 (Figure 4) show a gradual progression of increasing crystallinity; however, all the traces are very broad and the peaks are not well defined, with the exception of sample 7. The observed broad WAXS traces are indicative of the existence of either poorly formed crystallites or very small crystalline domains, which are insufficient in size to cause good X-ray diffraction.[2] The number and position of peaks developing in this series indicate that the predominant

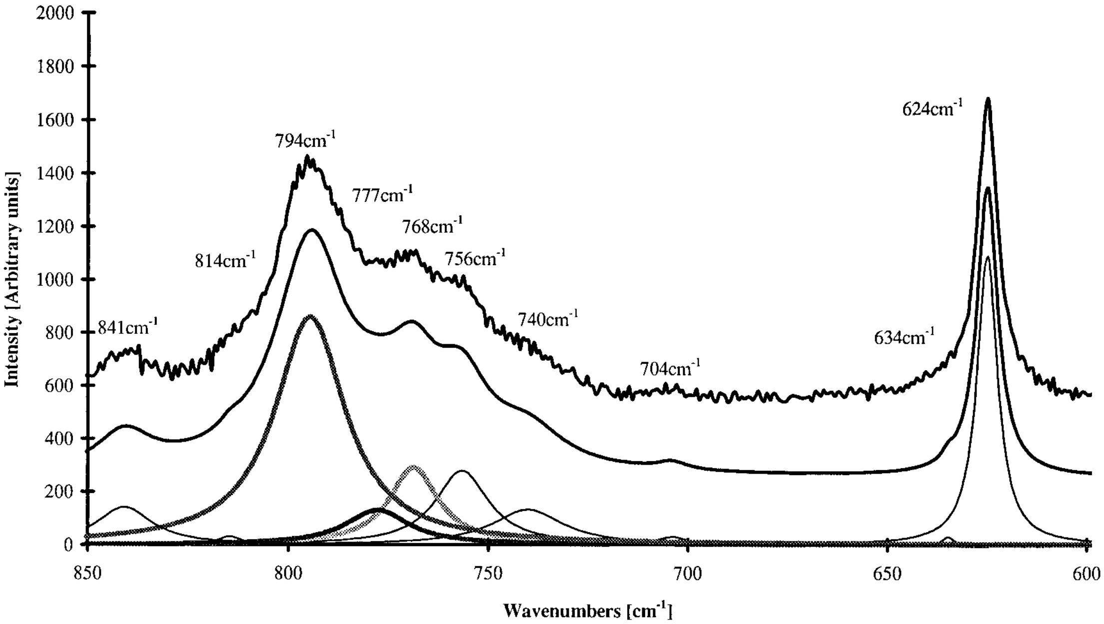

Figure 3. Fitted Raman spectrum of molten sPS.

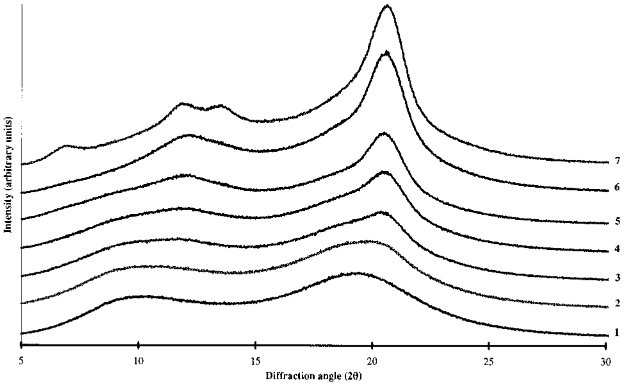

Figure 4. WAXS spectra of sPS films 1−7.

Table 2. Levels of Crystallinity for sPS Samples 1−7 As Determined by Raman, WAXS, DSC, and Infrared Spectroscopy/Sorption

		% crystallinity			
			DSC		infrared/
sample	$\%_{773}$	WAXS	20 °C/min	80 °C/min	sorption
1	10.9	0.0	20.0	14.0	6.4
2	13.4	4.0	26.0	17.0	11.2
3	21.9	8.5	38.0	30.0	18.6
4	30.4	8.2	46.0	39.0	23.9
5	41.4	12.0	53.0	51.0	38.3
6	46.9	38.6	56.0	54.0	44.7
7	53.6	53.0	50.0	45.0	47.9

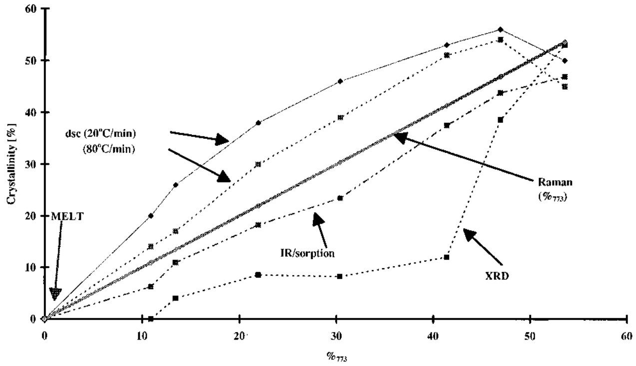

Figure 5. Comparison of various methods for the determination of crystallinity of sPS with that of the Raman analysis method.

crystal structure present is of the α form. Such broad spectra make determination of degree of crystallinity very difficult as it is not possible to determine accurately the background (amorphous) halo; the remaining peaks are so broad that area determination is often overestimated. The predicted "amorphous" background, for subtraction, is generated by computer software, based on the spectrum of the control sample (no. 1).

The crystallinity values derived from WAXS are given in Table 2 and are plotted against the adjusted value for $\%_{773}$ in Figure 5. The change in crystallinity as evidenced from the Raman data is not paralleled by the calculated WAXS values (Figure 5); an initial small increase is present followed by little change for samples 3, 4, and 5 and then a rapid increase for the last two films. For sample 7 there appears to be a close agreement between the X-ray diffraction value and that of the LRS; however, this is thought to be a coincidence, as the crystalline peaks are so diffuse in the WAXS spectra and cannot be taken as genuine measures of crystallinity. Obviously, the X-ray diffraction technique of measuring crystallinity quantitatively in these samples is totally inadequate, as one would expect for samples of low crystallinity and crystallite perfection. However, the spectra do indicate that there is an increase in crystalline order and perfection with annealing time. Most significantly, the values serve to show the problem of using this method for low crystalline volume fraction determination.

Differential Scanning Calorimetry (DSC). The DSC traces of the seven sPS films scanned at 20 and 80 °C/min are presented in Figures 6 and 7, respectively. Both scan rates reveal the same characteristic changes for a progressively more crystalline polymer. This is particularly evident for the first four specimens, where an exotherm arising from crystallization of the amorphous phase is seen to decrease in intensity and its peak to shift from ~157 to ~147 °C. The reduction in exothermic peak temperature is expected to be a result of seed nuclei. As the "amorphous" polymer is annealed for longer periods of time, more nucleation sites are formed. During the reheating cycle the cold crystal-

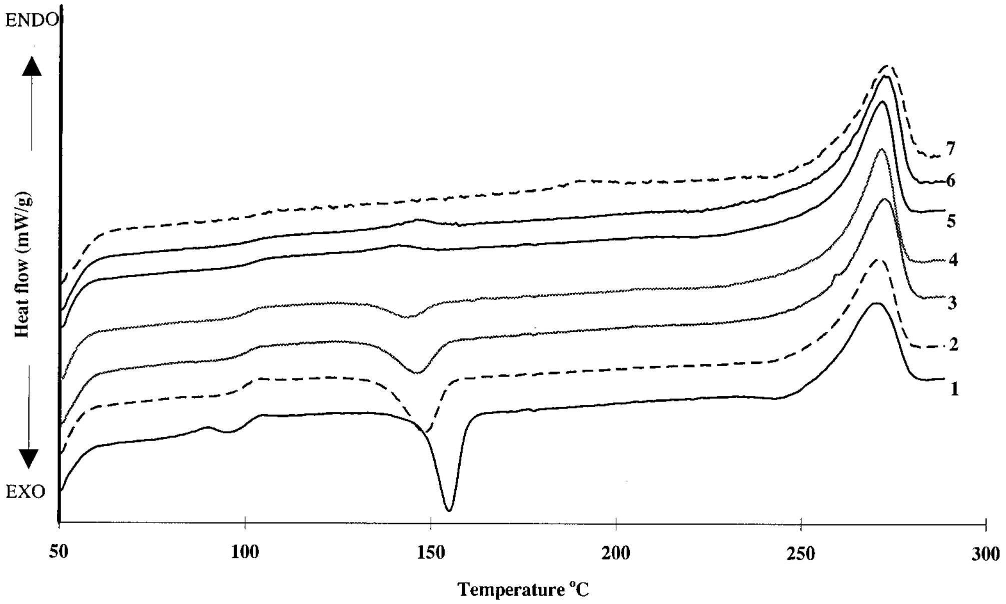

Figure 6. DSC traces of sPS films 1−7 (scan rate = 20 °C/min).

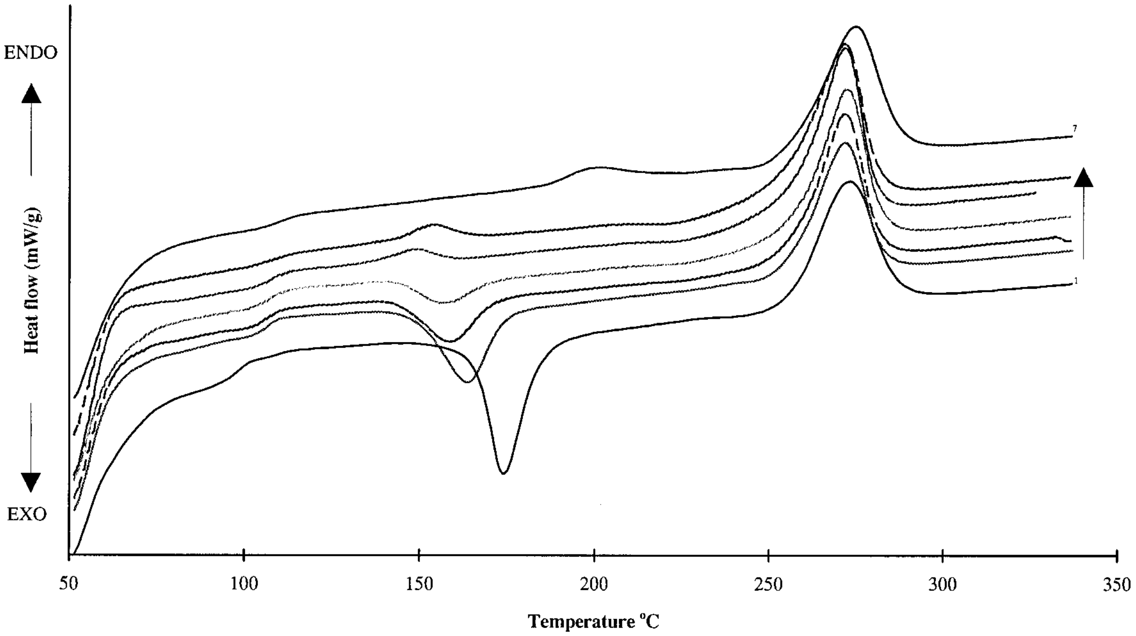

Figure 7. DSC traces of sPS fims 1−7 (scan rate = 80 °C/min).

lization temperature decreases with increase nucleation sites.

For samples 5, 6, and 7 a small broad endotherm appears, which shifts up in temperature with annealing time and temperature. The formation of a low-temperature endotherm approximately 10 °C above the crystallization temperature has been seen in a number of other semicrystalline polymers.[8,37−44] The explanation for its appearance is still a source of contention and, as pointed out by Vaughan and Stevens,[44] a number of different interpretations have been proposed.

The crystallinity values derived from these traces are given in Table 2 and a comparison between these data and the $\%_{773}$ is plotted in Figure 5. Both sets of DSC data give almost linear curves through the origin at higher values than those obtained from Raman or WAXS. The crystallinity values derived from the more rapid heating cycle are lower than those obtained at a heating rate of 20 °C/min, thus confirming other workers' data that low scan rates result in a higher level of apparent crystallinity[6] as a direct result of recrystallization during the heating cycle. Recrystallization during the DSC heating cycle can account for some, if not all, of the observed higher than expected crystallinity values for samples 1−6. However, the value of crystallinity obtained from sample 7 presents a marked deviation from the general trend. These "low" values were at first thought to be due to experimental error. Therefore, a new sample 7 was made and rerun. No significant difference in crystallinity was found between the two samples; therefore, the observed trend was accepted to be a true phenomenon. Recent experimental work has shown that there is a large difference in the morphologies present when amorphous samples of sPS are isothermally crystallized either at 120 or 145 °C.[35] In fact, at a constant crystallization time of 2 h, there is a decrease in the measured heat of fusion with increase in crystallization temperature from 120 to 145 °C. Then there is a gradual rise in heat of fusion as the temperature increases from 150 to 190 °C. This is

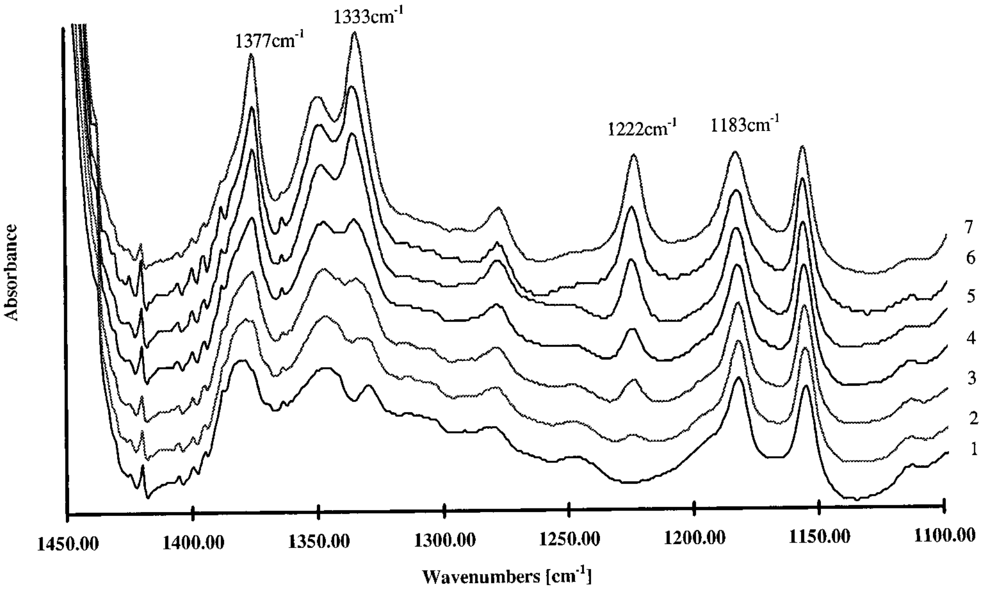

Figure 8. FTIR spectra of sPS films 1–7.

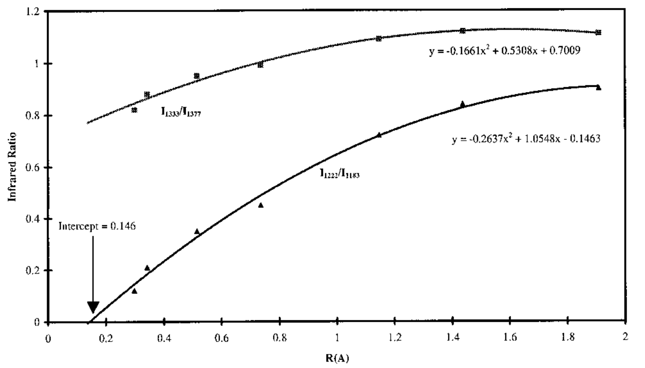

Figure 9. Comparison between the IR intensity ratio and $R(A)$ for different IR peaks as a function of increasing crystallinity.

obviously a very important result, and its interpretation will be discussed in a future publication.[35]

Infrared Spectroscopy (IR). Two research groups have recently reported different spectral features which can be used to determine crystallinity for sPS. Vittoria et al.[10] identify the 1222 cm^{-1} peak as being crystallinity sensitive and use the peak centered around 1183 cm^{-1} as a reference feature, whereas Lopez et al.[34] use the 1333 cm^{-1} band with the 1377 cm^{-1} peak as a reference. It was decided to analyze both pairs of peaks and compare the results with the Raman ν_1 ratio, $R(A)$. The series of infrared spectra are presented in Figure 8 and the two IR peak ratios, $I_{1333/1377}$ and $I_{1222/1183}$, are plotted as a function of $R(A)$ in Figure 9. The $I_{1222/1183}$ parameter employed by Vittoria et al.[10] relates to $R(A)$ via a second-order polynomial fit (Figure 9) with an intercept of 0.15. Similarly, a second-order polynomial curve can be fitted to the $I_{1333/1377}$ ratio employed by Lopez et al.[34] but the fit is much poorer with a low gradient. Hence, it seems that the infrared ratio $I_{1222/1183}$ used by Vittoria et al.[10] is a much more satisfactory qualitative estimate of crystallinity. Another interesting point is that the intercept value of $R(A)$ made by $I_{1222/1183}$ is very similar to that obtained for molten sPS—within experimental error—which is again consistent with the idea of a residual all-*trans* conformation within the melt.

Use of the linear relationship derived by Vittoria,[10] whereby infrared data can be correlated to percent crystallinity through the use of solvent sorption methods, enables an alternative value of crystallinity to be calculated for the various annealed film samples. For comparison, these data are plotted in Figure 5. A good correlation is observed between both vibrational techniques. However, the crystallinity values obtained are consistently ~4% lower than that determined by Raman spectroscopy (eq 1) but this is to be expected, as some "crystalline" interphase regions would be lost due to solvent interaction. Despite this slight deficit, the infrared/solvent data show a much closer relation to the $\%_{773}$ parameter defined by Raman measurements (eq 2) than any of the other established techniques.

Conclusions

This study has shown that by careful curve fitting and subsequent analysis of the Raman spectrum of sPS, the ν_1 vibrational mode can be assigned to two distinct features (three in the melt) which have been identified as being unique to either all-*trans* or *trans*/*gauche* conformations within the backbone. Furthermore, it has been shown that the total intensity of these features remains almost constant, enabling a quantitative measure of the molecular conformations to be made. Study of the spectrum obtained from molten sPS has shown that a residual quantity of the all-*trans* conformation is still present, despite the amorphous state of the material. When this "background" is taken into account, it is possible to use the $\%_{773}$ value as a quantitative measure of molecular crystallinity present within the sample. This assumption has been tested by comparing the $\%_{773}$ value with crystallinity values obtained from other established methods such as DSC and WAXS and from qualitative infrared/sorption data. The closest correlation for all the samples tested was obtained from infrared studies, where a relationship with solvent uptake was used to determine the amount of crystalline material present. The DSC measurements agreed well with those obtained by means of laser Raman spectroscopy. However, the DSC values were shown to be affected by scanning rate and by the thermal history of the material, often giving an overestimate of crystallinity. WAXS studies, on the other hand, were shown to be extremely poor at estimating low crystallinity levels.

It has therefore been demonstrated that for isotropic samples of sPS, Raman analysis can be used as an extremely effective method to determine crystallinity levels. It has the advantages of requiring little sample preparation, being nondestructive, and being fast; it is also insensitive to previous thermal history (i.e., melt crystallized or annealed) and through the use of fiber optics can be carried out on any sample regardless of size or location. Raman spectroscopy is also extremely sensitive to material anisotropy, and the ν_1 vibrational mode has excellent potential to provide information relating to the degree of orientation as well as level of crystallinity. Studies investigating this relationship will be reported in the third paper of these series.[35]

Acknowledgment. The authors would like to express their thanks to Mike Cook and Thomas Wegman (Dow Chemicals, Terneuzen, Holland) and Craig Carriere and Zhan Sun (Dow Chemicals, Midland, MI) for useful discussions and for supplying the materials of this work.

References and Notes

(1) Moore, S. *Mod. Plast. Int.* **1992**, Nov, 22.
(2) Alexander, L. E. *X-ray Diffraction Methods in Polymer Science*; Wiley-Interscience: New York, 1969.
(3) Balta-Calleja, F. J.; Vonk, C. G. *X-ray Scattering of Synthetic Polymers*; Elsevier: Oxford, 1989.
(4) Arnauts, J.; Berghmans, H. *Polym. Commun.*, **1990**, *31*, 343.
(5) Krzystowczyk, D. H.; Niu, X.; Wesson, R. D.; Collier, J. R. *Polym. Bull.* **1994**, *33*, 109.
(6) De Rosa, C.; Rapaccinolo, M.; Guerra, G.; Petraccone, V.; Corrandini, P. *Polymer* **1992**, *33*, 1423.
(7) Passingham, C.; Hendra, P. J.; Cudby, M. E.; Zichy, V.; Weller, M. *Eur. Polym. J.* **1990**, *26*, 631.
(8) Al Raheil, I. A. M. *Polym. Int.* **1994**, *35*, 189.
(9) Schultz, J. *Polymer Material Science*; Prentice Science: Englewood Cliffs, NJ, 1974.
(10) Vittoria, V.; Ruvolo Filho, A.; De Candia, F. *J. Macromol. Sci., Phys.* **1990**, *B29*, 411.
(11) Strobl, G. R.; Hagedorn, W. *J. Polym. Sci., Polym. Phys. Ed.* **1978**, *16*, 1181.
(12) Ward, I. M. *Chem. Ind. London* **1956**, 905; **1957**, 1102.
(13) Edwards, H. G. M.; Johnson, A. F.; Lewis, I. R. *J. Raman. Spectrosc.* **1993**, *24*, 475.
(14) Rodriguez-Cabello, J. C.; Quintanilla, L.; Pastor, J. M. *J. Raman Spectrosc.* **1994**, *24*, 335.
(15) Zerbi, G. *Appl. Spectrosc. Rev.* **1969**, *2*, 193.
(16) Jawhari, T.; Quintanilla, L.; Pastor, J. M. *J. Appl. Polym. Sci.* **1994**, *51*, 463.
(17) Naylor, C. C.; Meier, R. J.; Kip, B. J.; Williams, K. P. J.; Mason, S. M.; Conroy, N.; Gerrard, D. L. *Macromolecules* **1995**, *28*, 2969.
(18) Mutter, R.; Stille, W.; Strobl, G. *J. Polym. Sci., B: Polym. Phys.* **1993**, *31*, 99.
(19) Rull, F.; Prieto, A. C.; Casado, J. M.; Sobron, F.; Edwards, H. G. M. *J. Raman Spectrosc.* **1993**, *24*, 545.
(20) Ishihara, N.; Seimiya, T.; Kuramoto, M.; Voi, M. *Macromolecules* **1986**, *19*, 2464.
(21) Guerra, G.; Vitagliano, V. M.; De Rosa, C.; Petraccone, V.; Corradini, P. *Macromolecules* **1990**, *23*, 1539.
(22) Corradini, P.; Guerra, G. *Adv. Polym. Sci.* **1992**, *100*, 183.
(23) Doherty, D. C.; Hopfinger, A. J. *Macromolecules* **1989**, *22*, 2472.
(24) Reynolds, N. M.; Savage, J. D.; Hsu, S. L. *Macromolecules* **1989**, *22*, 2867.
(25) Filho, A. R.; Vittoria, V. *Makromol. Chem., Rapid Commun.* **1990**, *11*, 199. Guerra, G.; Musto, P.; Karasz, F. E.; MacKnight, W. J. *Makromol. Chem.* **1990**, *191*, 2111.
(26) Nakaoki, T.; Kobayashi, M. *J. Mol. Struct.* **1991**, *242*, 315.
(27) Kobayashi, M.; Nakaoki, T.; Ishihara, N. *Macromolecules* **1990**, *23*, 78.
(28) Reynolds, N. M.; Stidham, H. D.; Hsu, S. L. *Macromolecules* **1991**, *24*, 3662.
(29) Reynolds, N. M.; Hsu, S. L. *Macromolecules* **1990**, *23*, 3463.
(30) Nyquist, R. A.; Putzig, C. L.; Leugers, M. A.; McLachlan, R. D.; Thill, B. *Appl. Spectrosc.* **1992**, *46*, 981.
(31) Kobayashi, M.; Nakaoki, T.; Ishihara, N. *Macromolecules* **1989**, *22*, 4377.
(32) Kellar, E. J. C.; Galiotis, C.; Andrews, E. H. *Macromolecules* **1996**, *29*, 3515.
(33) Jasse, B.; Chao, R. S.; Koenig, J. L. *J. Raman Spectrosc.* **1979**, *8*, 244.
(34) Lopez, L. C.; Cieslinksi, R. C.; Putzig, C. L.; Wesson, R. D. *Polymer* **1995**, *36*, 2331.
(35) Evans, A. M.; Kellar, E. J. C.; Galiotis, C.; Andrews, E. H., to be published.
(36) Pasztor, J. R.; Landes, B. G.; Karjala, P. J. *Thermochim. Acta* **1991**, *177*, 187.
(37) Wunderlich, B. *Macromolecular Physics*; Academic Press: New York, 1980; Vol. 3.
(38) Lemstra, P. J.; Kooistra, T.; Challa, G. *J. Polym. Sci., Part A-2*, **1972**, *10*, 823.
(39) Blundell, D. J.; Osborn, B. N. *Polymer* **1983**, *24*, 953.
(40) Chixing, Z.; Clough, S. B. *Polym. Eng. Sci.* **1988**, *28*, 65.
(41) Bassett, D. C.; Olley, R. H.; Al Raheil, I. A. M. *Polymer* **1988**, *29*, 1745.
(42) Lee, Y.; Porter, R. S. *Macromolecules* **1987**, *20*, 1336.
(43) Passingham, C.; Hendra, P. J.; Cudby, M. E.; Zichy, V.; Weller, M. *Eur. Polym. J.* **1990**, *26*, 31.
(44) Vaughan, A. S.; Stevens, G. C. *Polymer* **1995**, *36*, 1531.

MA961136D